

# IMPACT OF INTERACTIVE PHYSICAL RETRIEVALS ON NWP

Joel Susskind and James Pfaendtner  
Laboratory for Atmospheres  
NASA Goddard Space Flight Center  
Greenbelt, MD, U.S.A.

Summary: Forecast impact results with the GLA interactive forecast-retrieval-assimilation system, which directly uses satellite radiance data in the assimilation cycle, are presented. Forecasts made from initial conditions derived with this system are shown to be more skillful than those whose initial conditions came from a comparable assimilation using statistically based temperature soundings, or ones using no sounding data at all. Examples are also given of additional parameters which are produced through the physical inversion of the satellite radiance data during the interactive assimilation cycle. These are potentially useful for analysis purposes.

## 1. INTRODUCTION

The Global Modeling and Simulation Branch of the Goddard Laboratory for Atmospheres (GLA) has had an active research program in satellite retrieval methods and data assimilation technique development for a number of years (Ghil et al., 1979; Atlas et al., 1982; Baker, 1983; Baker et al., 1984; Baker et al., 1987; Susskind et al., 1984; Susskind and Reuter, 1985; Susskind et al., 1987b; Kalnay et al., 1985). The special emphasis of the GLA research program has been and continues to be the optimal utilization of observations from space-based instruments. Global data assimilation, the genesis of which can be found in the paper by Charney, Halem and Jastrow (1969), is now used by all operational forecasting centers for NWP applications. In recent work at GLA, (Susskind et al., 1987b), the retrieval process, in which geophysical parameters are obtained from satellite observations, has been integrated into a global data assimilation cycle. Two benefits are expected from this direct interactive use of satellite data. First, the a priori information from all relevant sources contained in the first guess fields produced by the assimilation system will improve the accuracy of all retrieved parameters. Assimilating these more

accurate soundings will in turn improve the quality of the analysed fields and subsequent forecasts. The second benefit to be derived from the interactive system follows directly from the physical basis of the GLA retrieval algorithm. In contrast to statistically based methods, physical retrievals necessarily entail solving for an entire set of atmospheric and surface parameters simultaneously. These "extra" parameters (sea surface temperature, land surface temperature, effective cloud cover, cloud top height, snow and ice extent, total ozone burden, outgoing longwave radiation, precipitation estimate) open the possibility for important new applications of the data assimilation process. The internal consistency of the retrieval process can be verified by comparing these parameters to ones derived from other independent data. The physical parameterizations in models can be more directly verified through the use of these parameters. And importantly, longer time series of internally consistent parameters, produced as part of the data assimilation process, will have valuable applications in environmental monitoring and earth system science. Some recent results from the GLA interactive system, in terms of both forecast impact and the derived geophysical parameters, are presented in this paper.

The GLA physical inversion retrieval method uses radiance data (19 infra-red channels from the HIRS2 instrument plus 4 complementary microwave channels from MSU) from the NOAA polar orbiter series of satellites to derive temperature-humidity profiles. Moreover, as was mentioned above, the retrieval algorithm determines global fields of sea-land surface temperature as well as global cloud and ozone fields and estimates of precipitation and ice/snow cover. Data assimilations using the retrieved temperature profiles have led to significantly improved 3-6 day forecast skill (Baker, et al., 1984, Kalnay et al., 1985; Susskind et al., 1987b).

The next section contains a broader description of the GLA retrieval algorithm, and section 3 describes the interactive forecast-retrieval-assimilation system. Section 4 contains the results from recent forecast impact tests, while section 5 discusses the additional parameters obtained through the interactive cycle and presents some examples. Section 6 indicates plans for future research.

## 2. THE GLA PHYSICAL INVERSION RETRIEVALS

Physical retrieval methods (those in which the radiative transfer equation is directly solved to obtain a match with the observed radiance data) have a number of important advantages over statistically based methods. Physical methods allow a direct incorporation of all factors affecting the radiances such as surface properties, scan angle of observation, and most importantly, clouds. As shown in Susskind et al. (1984), the GLA physical retrieval scheme produces temperature soundings whose accuracy does not appreciably deteriorate with increasing cloudiness, and current studies have shown that there is also no significant degradation at large satellite angles. In addition, surface parameters and cloud information are determined from the data in the physical system. The geophysical parameters determined from the observed radiances are given a quality weight according to the agreement of observed and computed brightness temperatures, and solutions (other than cloud parameters) are "rejected" if sufficient agreement cannot be found. Moreover, the ability to compute radiances from the forecast first guess and compare with satellite observations provides a powerful tool to assign a quality indicator to the first guess field for use in the assimilation cycle.

The basic retrieval method is described in Susskind et al. (1984). In order to perform accurate physically based retrievals, it is essential to compute the radiances which the instrument would see as a function of the atmospheric and surface conditions with sufficient accuracy. The details of the calculation of channel averaged radiances as a function of atmospheric temperature-humidity-ozone profiles, surface temperature, surface elevation, surface emissivity, and zenith angle of observation, are described in Susskind et al. (1983). An updated cloud filtering algorithm and improved method for determining land/sea surface temperature appeared in Susskind and Reuter (1985). Improvements in the determination of cloud parameters are described in Susskind et al. (1987a). The algorithm for humidity retrievals is detailed in Reuter et al. (1988).

The physically retrieved temperature profiles arise as solutions to a variational problem in which the radiative transfer equation is used to compute radiances which are then compared in an objective function

defined in terms of the observed (that is, cloud corrected) radiances. Successful retrievals using all the observed data can be performed under most cloud conditions, and "microwave only" retrievals are never performed. The retrieval process is underdetermined (there is no unique solution), and highly non-linear, especially with respect to assumed cloud amount and distribution. Hence, another advantage of physical retrievals is their ability to take advantage of additional first-guess information.

Any information in the first guess can potentially be of great value to the retrieval algorithm because of the indeterminateness of the problem. On the other hand, the possibility that the retrieval algorithm could be seriously led astray by errors in the first guess needs to be examined. A good retrieval scheme can be characterized by its ability to improve an inaccurate first guess significantly while only making slight changes in those cases where the guess is accurate. Reuter *et al.* (1988) examined the first guess dependence of the GLA physical temperature retrievals and found them to have the aforementioned desirable characteristics.

### 3. THE GLA INTERACTIVE FORECAST-RETRIEVAL-ANALYSIS CYCLE

The GLA interactive forecast-retrieval-analysis cycle combines three basic steps, a forecast model, a module for inverting satellite data, and a procedure to give the current best estimate of the state of the atmosphere given all available information. In each 6-hour period, the interactive cycle starts with the 6-hour forecast fields generated by the GLA Fourth Order GCM (Kalnay, *et al.*, 1983). The vertical structure from these 6-hour temperature and humidity fields is used as an initial guess to generate retrievals for all soundings occurring in the interval  $\pm 3$  hours of the forecast time. A successive correction (SCM) analysis (Baker, 1983) is then used to assimilate the generated retrievals and all other observations (such as radiosonde and ship reports, etc.) made during the  $\pm 3$ -hour interval. A 6-hour forecast, using the analysis just generated for initial conditions, then completes the cycle. While a number of geophysical parameters are retrieved along with the temperature profiles, only the thicknesses from the retrieved temperatures are being used in the data

assimilation at this time. In addition, we have not yet utilized the quality indicator of the first guess, given by the agreement of observed brightness temperatures with those computed from the guess, in the analysis procedure.

Our experience with this system indicates that using the same first guess for both the physical retrievals and the data assimilation is advantageous to both subsystems. Some of the benefits to the retrievals were discussed in the previous section. The advantage for the analysis and subsequent forecasts is that whenever the first guess is accurate, retrievals do not significantly alter the guess and modifications made by the analysis are small, thus maintaining the dynamic balance of the model. Moreover, after a few days, an equilibrium is reached in the interactive cycle and changes to the first guess become small almost everywhere. This produces less noise in the analyzed fields and also limits the problems of "edge effects." Of course the use of a forecast first guess for the retrievals may lead to errors in the retrievals being correlated with errors in the first guess. While such error correlations were not accounted for by the SCM analysis used in the present interactive cycle, it would be relatively straightforward to incorporate them into a statistical optimal interpolation type analysis. It might be mentioned that preliminary computations with a two week sample of statistical retrievals collocated to radiosondes show their errors also to be correlated with first guess errors. Such correlations could arise if for example, both the retrievals and the prediction model and/or analysis scheme had a bias toward climatology.

The interactive system has been used to process data for the FGGE year, December 1978-December 1979, and also for the time periods July 1983 and August-September 1987. The latter period was processed in near real time (same day processing) in conjunction with the Antarctic ozone hole experiment. The period May-July 1988 is currently being processed preliminary to a joint study between GLA and the National Meteorological Center (NMC). Late in this study, physical retrievals will be generated using a first guess from the global prediction system at NMC. The retrievals will then be used in an experimental (non-interactive) reanalysis and forecast impact study to be done with the NMC system.

The use of physical retrievals in an interactive cycle offers many other opportunities for improving the quality of the resulting analyses. Two of these which will be pursued at GLA in the near future are: 1) use of the retrieved sea surface temperatures to perform a parallel analysis of sea surface temperature anomaly within the assimilation cycle, with the evolving SST analysis being used by the model as a lower boundary condition, and 2) use of the radiance data to assign quality weights to the first guess in those cases where the retrieval algorithm can clearly determine that the first guess is in error. These weights could be used to modify the forecast error variance estimates needed in optimal interpolation.

#### 4. FORECAST IMPACT EXPERIMENTS

Forecast impact experiments are a sensitive measure of the relative quality of various atmospheric analyses. For the FGGE year three analyses have been produced at GLA: 1) An assimilation using only conventional data - called NOSAT; 2) An analysis using all standard FGGE data including conventional data, the satellite soundings produced by NOAA NESDIS, satellite derived cloud track winds, and other special FGGE data such as buoys - called the Full FGGE; and 3) An interactive analysis using the same data as the Full FGGE except that the GLA interactive retrievals were used in place of the NESDIS soundings - called INTERACTIVE. All three assimilations used the "Final IIb" conventional data, the SCM analysis algorithm (which analyzes on 12 standard pressure levels), and the 4 deg. latitude by 5 deg. longitude, 9-level version of the GLA Fourth Order GCM.

Initial conditions for the forecasts were chosen every fourth day for a winter period (January 9, 1979 to March 5, 1979), and for a summer period (May 5, 1979 to June 30, 1979). The forecasts were performed using both the 4° x 5° version of the model, and a higher resolution, 2° x 2.5° 9-level version of the Fourth Order Model with initial conditions interpolated from the horizontally coarser analysis at the 12 standard pressure levels. All forecasts were verified against the ECMWF IIIb analysis for the FGGE year interpolated to the 4° x 5° grid.

Figures 1a and b show average anomaly correlation coefficients for sea level pressure for an ensemble of fifteen 5 day forecasts, run every 4th day from January 9, 1979 to March 5, 1979, using the  $2^{\circ} \times 2.5^{\circ}$  model. The anomaly correlation coefficients in Figures 1a and b are verified against ECMWF analyses over the entire Northern Hemisphere extra tropics (Figure 1a) and over North America (Figure 1b). As is customary, we will take an anomaly correlation coefficient of 0.6 as the limit of useful forecast skill.

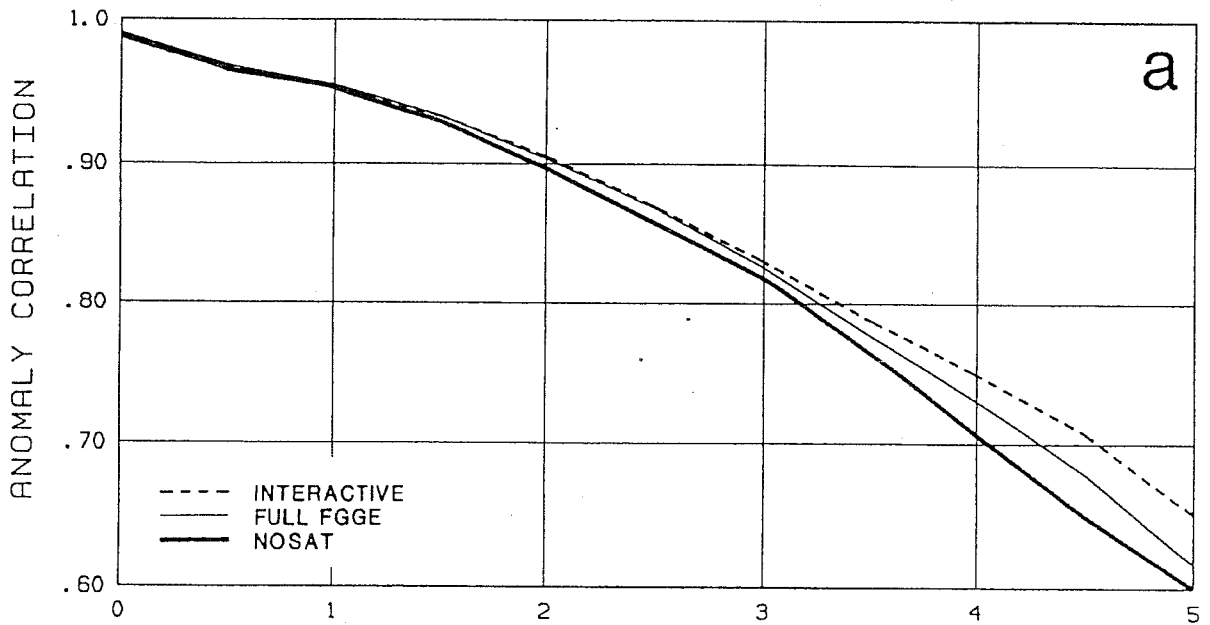
Figure 1a shows that the limit of skill of the NOSAT forecasts for the Northern Hemisphere is about 5 days, while the average skill, over the entire winter, of the Full FGGE forecasts appears to be greater by about 3 hours compared to that of NOSAT, and that of the GLA interactive forecasts by at least 12 hours. Figure 1b shows that the average skill of all sets of forecasts for North America is somewhat less than that of forecasts for the entire Northern Hemisphere. Nevertheless, we still observe an improvement of skill of the interactive forecasts, compared to the NOSAT forecasts, of more than 12 hours. This is in sharp contrast to the 3 hour negative impact of the Full FGGE forecasts compared to the NOSAT forecasts over North America.

In general, the  $2^{\circ} \times 2.5^{\circ}$  forecasts were more skillful than the  $4^{\circ} \times 5^{\circ}$  forecasts run from the same analyses, but the degree of improvement depended on the nature of the data used. Figure 2a shows the improvement in skill, due to model resolution, of the interactive forecasts of sea level pressure verified over the Northern Hemisphere extra-tropics, to be about 20 hours on the average. Figure 2b shows the improvement in skill, due to model resolution, of the NOSAT forecasts verified over the same region to be only about 12 hours. In general, forecasts from the Full FGGE analyses showed intermediate levels of improvement, between that of NOSAT and of the interactive forecasts, when model resolution was increased. This finding, which also held in other geographical areas, is a result of the higher resolution model being more sensitive to improvements in the initial conditions and the quality of the data entering into them. Consequently, increasing the spatial resolution of the model can increase the impact of satellite soundings on the forecast skill, especially if the soundings are compatible with the model. Figure 3

AVERAGE OF 15 2°x 2.5° FORECASTS JAN 9 - MAR 5, 1979

SEA LEVEL PRESSURE - NH. EXTRA TROPICS

LAT: 30N - 86N LONG: 0 - 355E



SEA LEVEL PRESSURE - NORTH AMERICA

LAT: 30N - 70N LONG: 130W - 75W

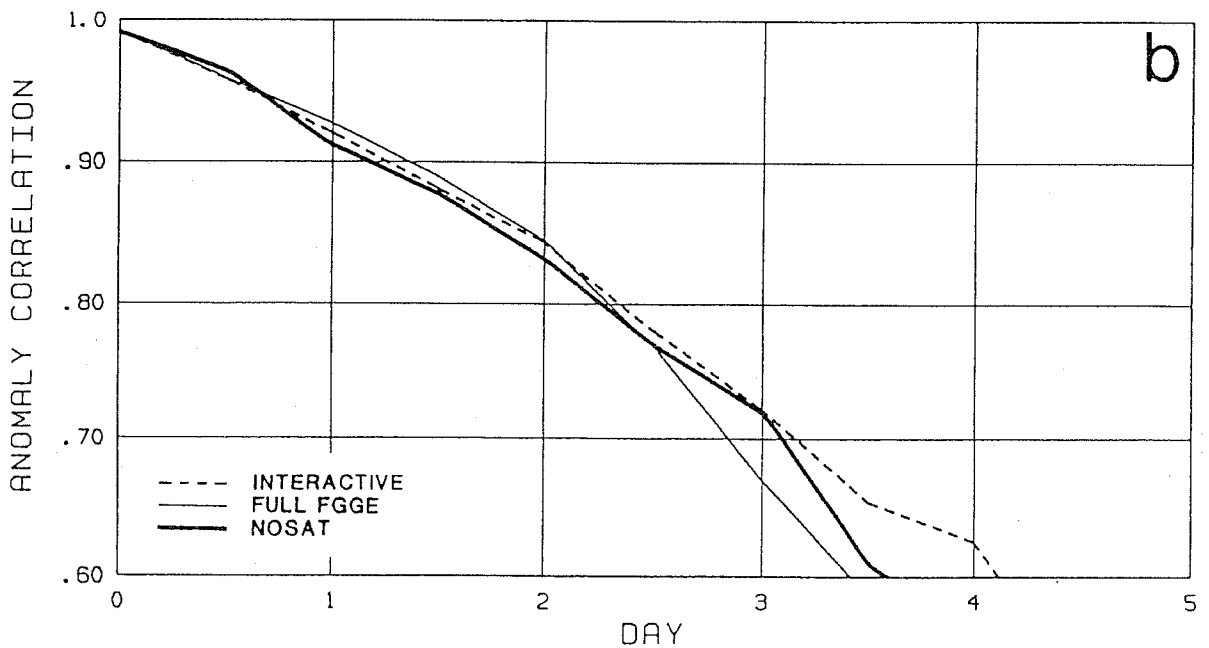


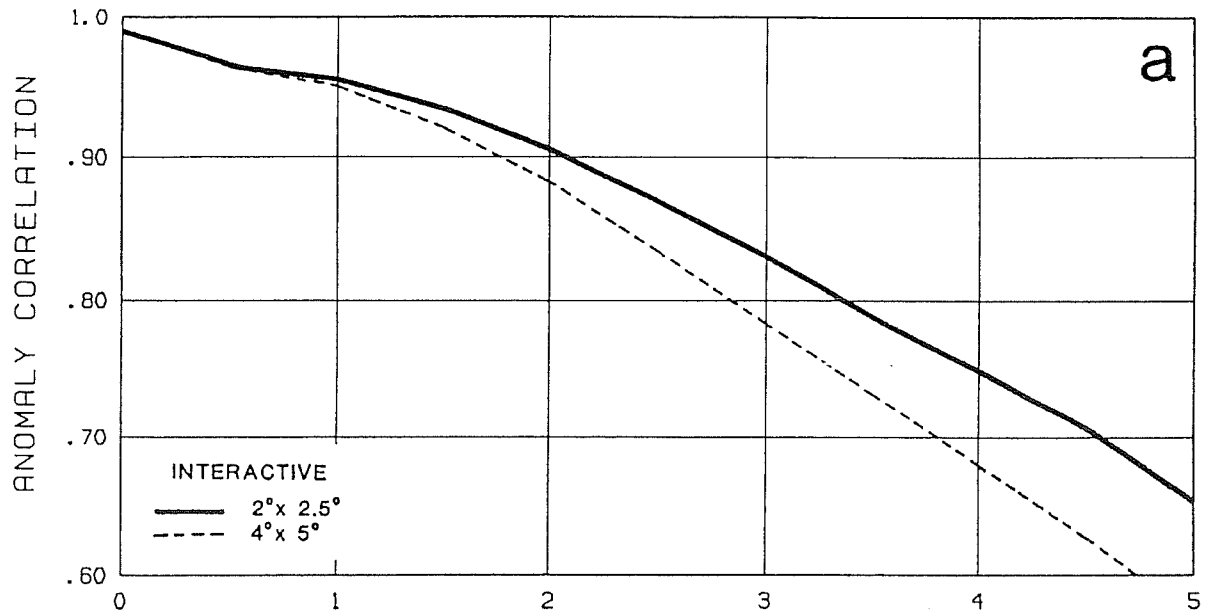
Figure 1 Average sea level pressure anomaly correlation coefficients, verified against the ECMWF analysis, for ensembles of 15 2°x2.5° 5-day forecasts from three 4°x5° SOP I assimilations.



AVERAGE OF 15 FORECASTS JAN 9 - MAR 5, 1979

SEA LEVEL PRESSURE - NH. EXTRA TROPICS

LAT: 30N - 86N LONG: 0 - 355E



SEA LEVEL PRESSURE - NH. EXTRA TROPICS

LAT: 30N - 86N LONG: 0 - 355E

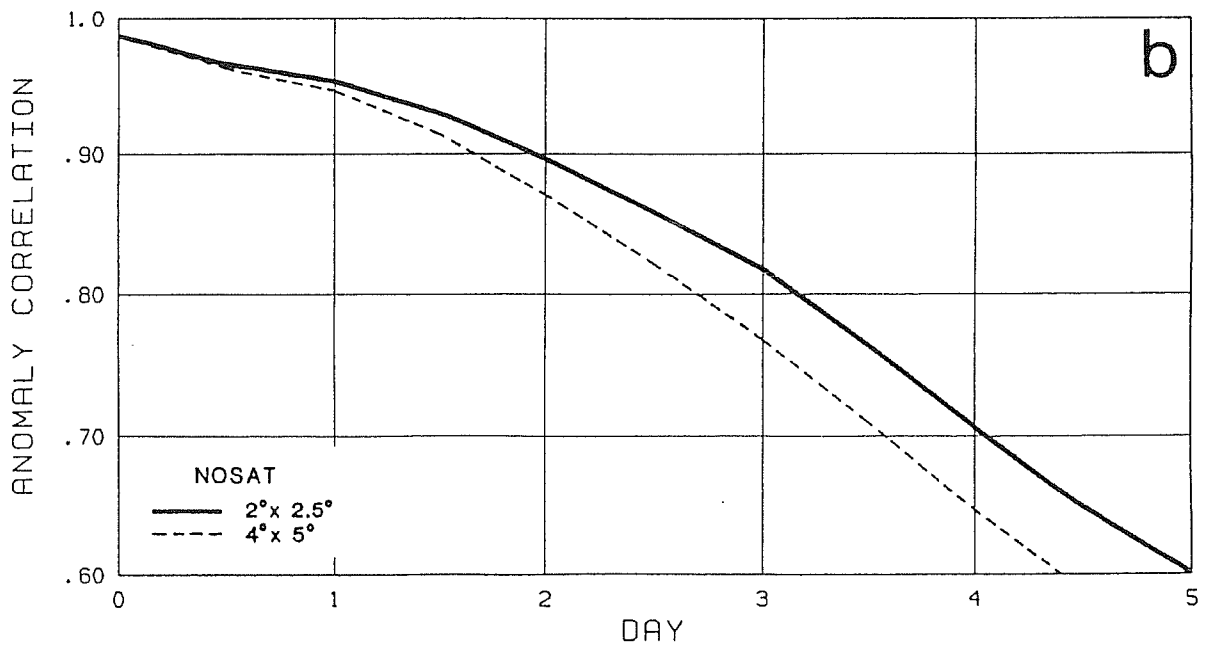


Figure 2 Forecast skill as a function of model resolution with initial conditions from two assimilations.

shows results from the ensemble of 15  $2^\circ \times 2.5^\circ$  forecasts in SOP II of FGGE. Improvement in forecast skill appears smaller in the summer than in the winter, but is still significant, especially over North America.

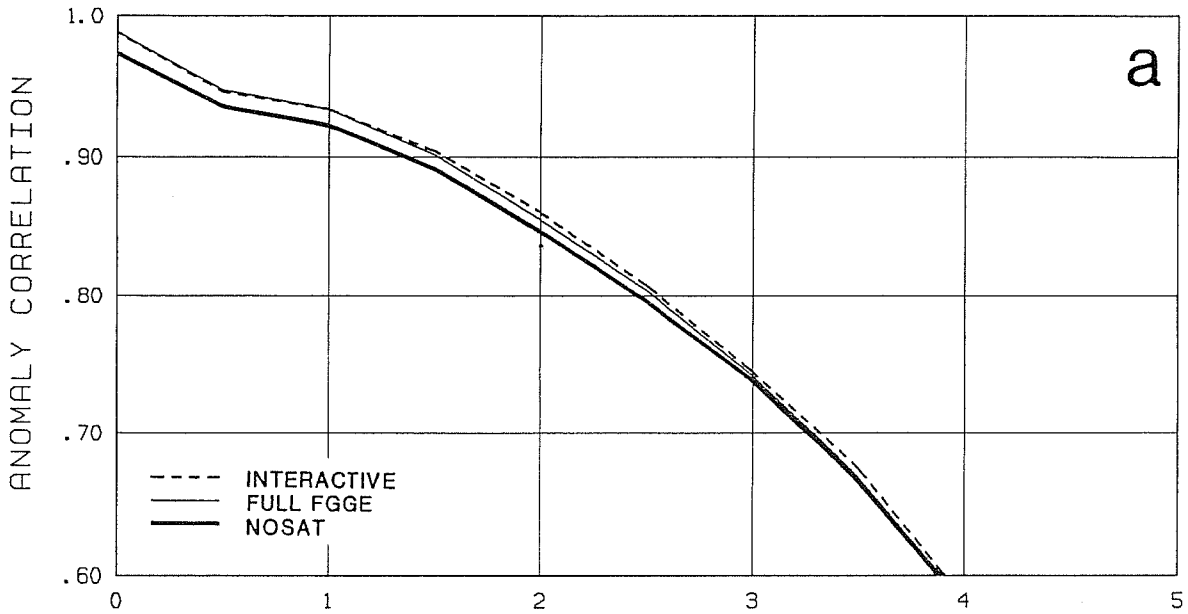
Using a slightly improved version of the physical retrieval algorithm, the interactive cycle has recently been used to analyze the period May 15, 1988 to July 15, 1988. A non-interactive assimilation using the same data, except for the omission of all satellite temperature soundings, has also been completed for the same period. The objective of the new test was to isolate the effect of inclusion of the satellite soundings into the analysis from additional effects of cloud track winds and other special sources of data, such as buoys. We will refer to this analysis as NO SAT TEMP. Note that the data types used in this second assimilation are not identical to those used for the NOSAT of the FGGE year, the most important difference probably being the exclusion of both satellite data and cloud motion winds from the NOSAT analysis. Eight forecasts with initial conditions chosen every four days from May 23, 1988 to June 20, 1988 have been done from each of these analyses. The forecast model used was identical to that used for the 1979 forecasts. The interactive analysis was used for forecast verifications because the ECMWF analysis was not available. Isolated tests using 1979 data showed only slight differences in verification statistics when forecasts were verified against the ECMWF analyses or the interactive analyses, with the largest differences occurring at zero time.

Figure 4 shows anomaly correlations for sea level pressure forecasts verified over the Northern Hemisphere extra tropics and North America made using the  $2^\circ \times 2.5^\circ$  version of the model from the interactive and NO SAT TEMP analyses. It is apparent from Figure 4a that almost a 12 hour improvement in forecast skill of sea level pressure for the Northern Hemisphere extra-tropics resulted from incorporation of the satellite data into the analyses in this summer period. This improvement is much larger than that found in SOP II of FGGE and comparable to the improvement found in the winter in SOP I of FGGE. A somewhat smaller improvement in skill for sea level pressure forecasts over North America is shown in Figure 4b. This improvement is roughly comparable to that seen in SOP II of FGGE for this region.

AVERAGE OF 15 2°x 2.5° FORECASTS MAY 5 - JUNE 30, 1979

SEA LEVEL PRESSURE - NH. EXTRA TROPICS

LAT: 30N - 86N LONG: 0 - 355E



SEA LEVEL PRESSURE - NORTH AMERICA

LAT: 30N - 70N LONG: 130W - 75W

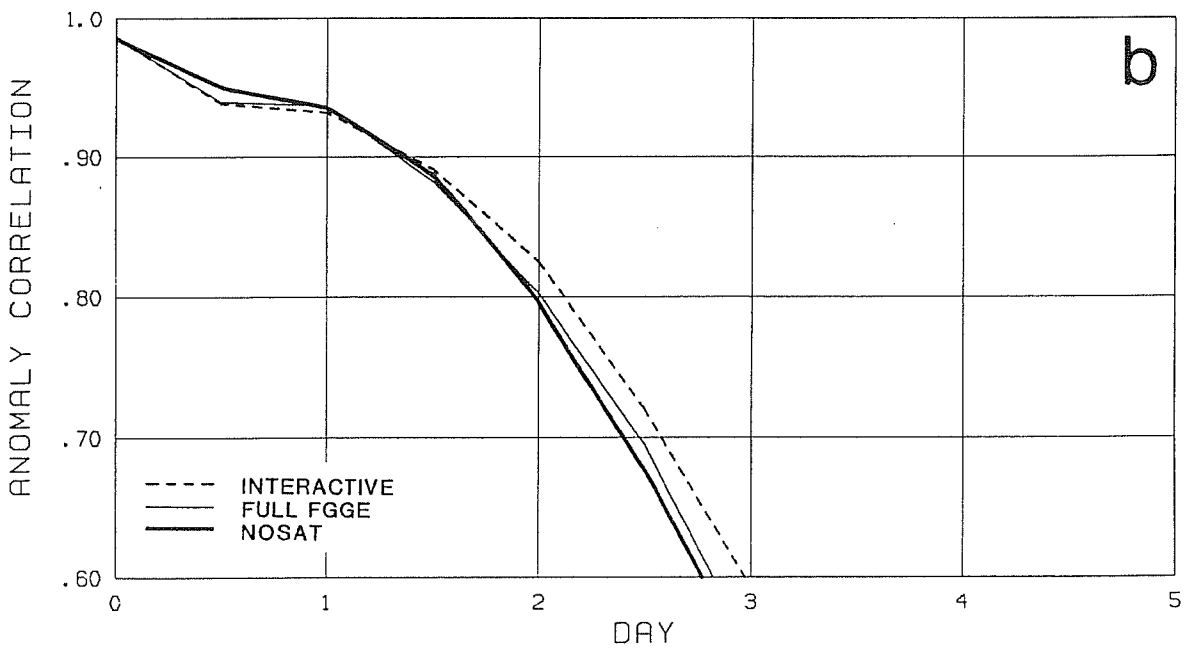
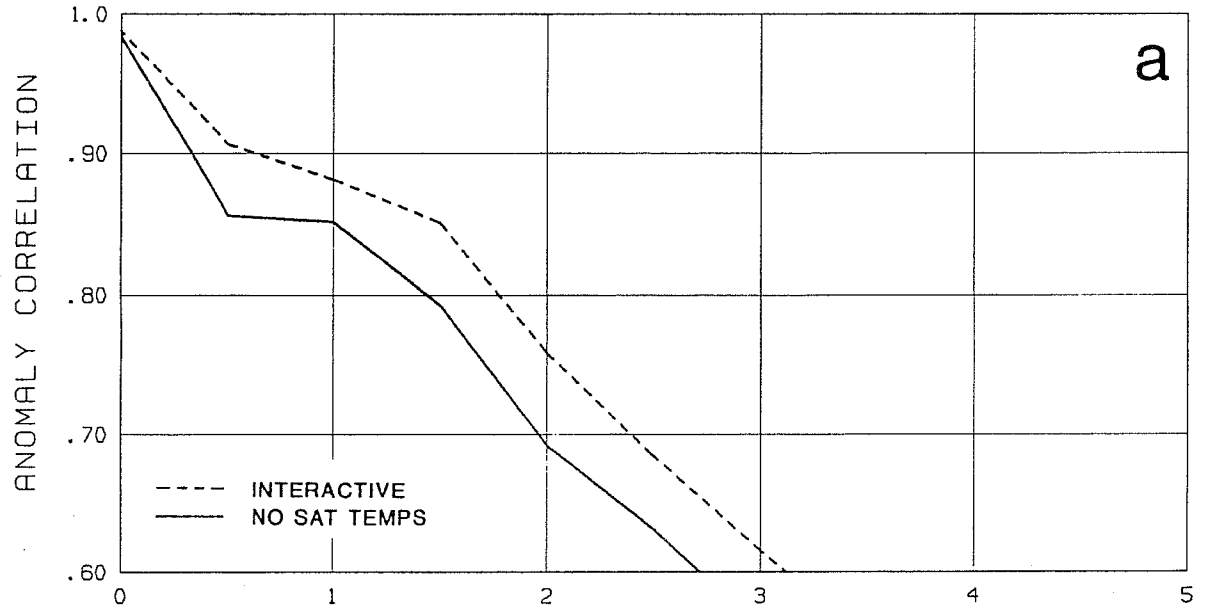


Figure 3 Average sea level pressure anomaly correlation coefficients of 15 2°x2.5° 5-day forecasts from three 4°x5° SOP II assimilations.

AVERAGE OF 8 2°x 2.5° FORECASTS MAY 23 - JUNE 20, 1988

SEA LEVEL PRESSURE - NH. EXTRA TROPICS

LAT: 30N - 86N LONG: 0 - 355E



SEA LEVEL PRESSURE - NORTH AMERICA

LAT: 30N - 70N LONG: 130W - 75W

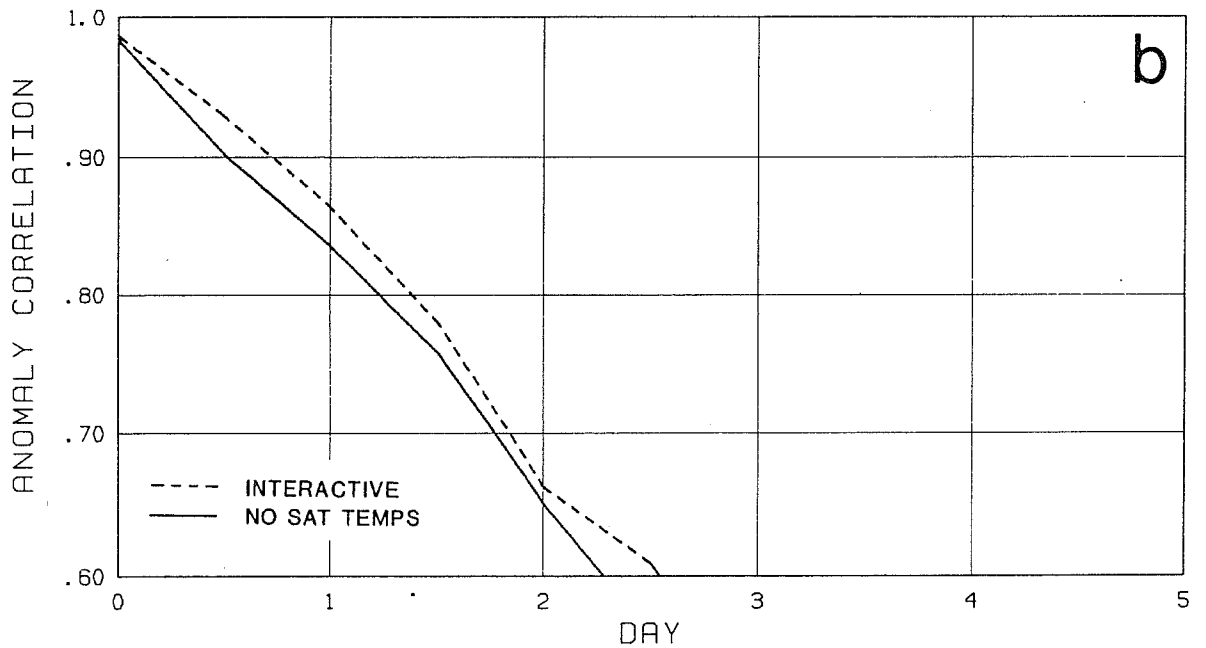
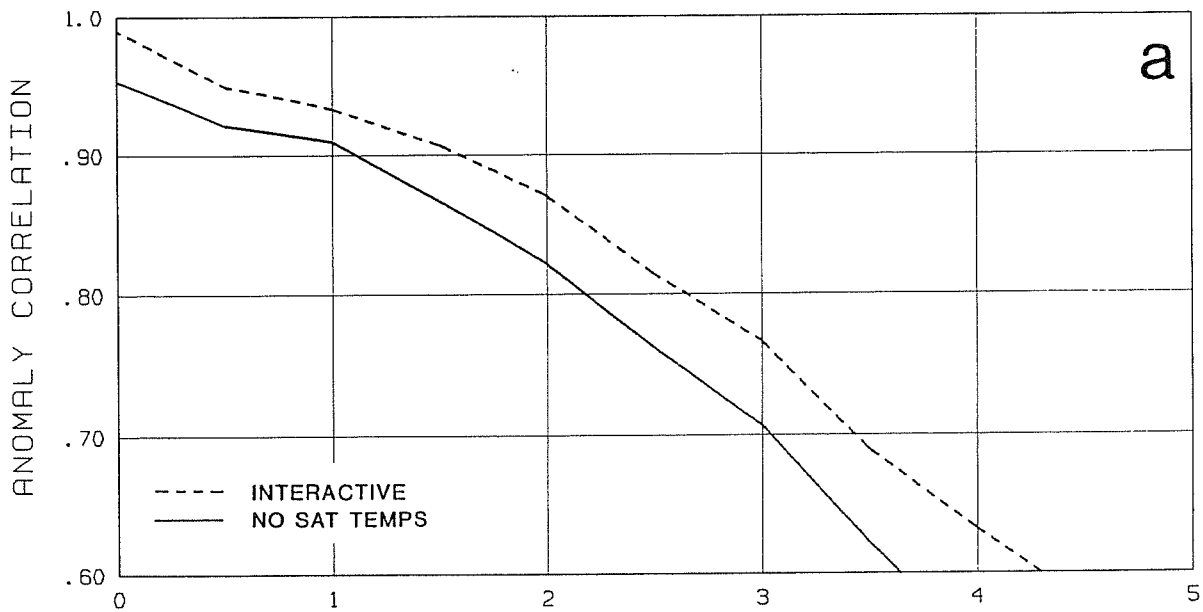


Figure 4 Average sea level pressure anomaly correlation coefficients, verified against the interactive analysis, for two ensembles of 8 1988 summer 2°x2.5° forecasts run from their respective 4°x5° assimilations.

AVERAGE OF 8 2°x 2.5° FORECASTS MAY 23 - JUNE 20, 1988

500 MB GEOPOTENTIAL HEIGHT - NH. EXTRA TROPICS

LAT: 30N - 86N LONG: 0 - 355E



500 MB GEOPOTENTIAL HEIGHT - NORTH AMERICA

LAT: 30N - 70N LONG: 130W - 75W

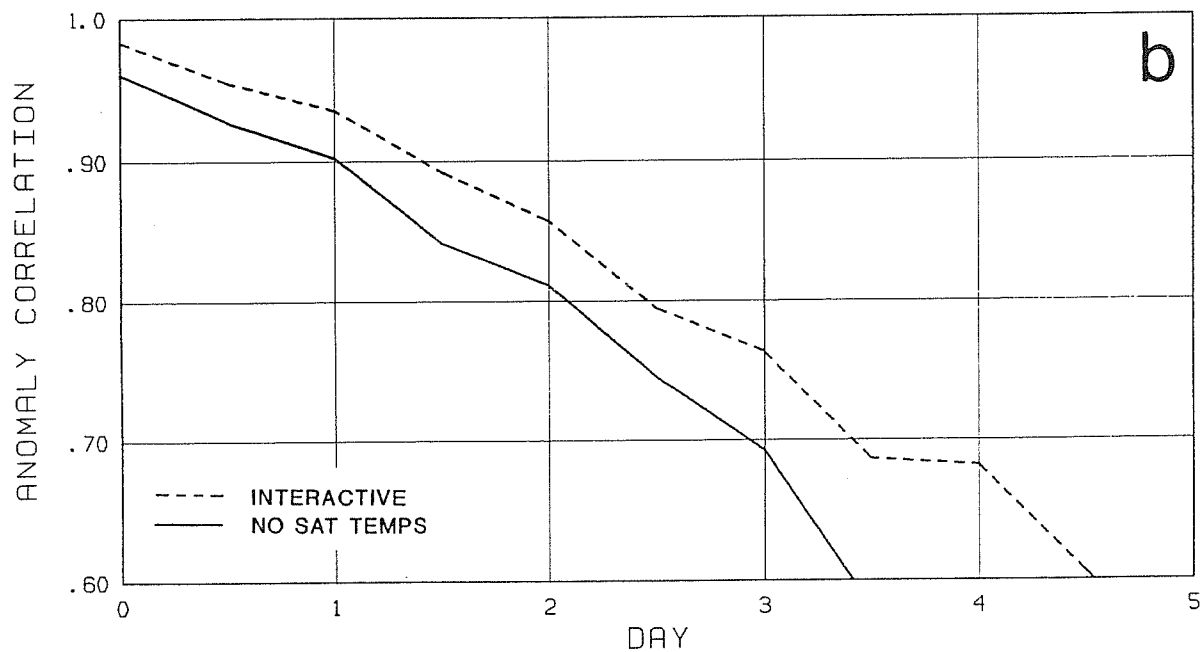


Figure 5 Average 500 mb height anomaly correlation coefficients, verified against the interactive analysis, for two ensembles of 8 1988 summer 2°x2.5° forecasts run from their respective 4°x5° assimilations

The improvements in forecast skill appear especially dramatic during this period when one examines the verification statistics for the 500 mb geopotential height, which are shown in Figure 5. The positive impacts over the Northern Hemisphere extra-tropics are more than 12 hours, and over North America are over 1 day. Some of the statistical improvement at zero time may be due to the artifact of verification against the interactive analysis, but this would have little effect at later time periods. It should be added that no negative impacts were observed in any of the eight forecasts in the ensemble. This large effect was not found in SOP II of FGGE.

There are a number of possible explanations for this difference in results. First of all, we are dealing with a different year and a different ensemble of situations. Second, there have been some improvements in the method used to analyze the satellite sounding data, compared to that used in the FGGE year, and this may have contributed to the improved impact. In addition, there is the added consideration that the NOSAT analyses in the FGGE year did not "enjoy the benefit" (or should we say "suffer the detriment") of the cloud track winds, which were used in the interactive analyses. To test this effect, we are now performing an analysis for the 1988 period in which both satellite temperatures and cloud track winds are withheld from the analysis to determine the effect of including the cloud track winds in the analysis. If the new forecasts are significantly improved over those from the NO SAT TEMP analysis, we will do an additional test, deleting the cloud track winds from the interactive analysis as well.

##### 5. ADDITIONAL PARAMETERS FROM THE GLA RETRIEVALS

The GLA physically based method is used to analyze HIRS2/MSU data to produce atmospheric temperature and humidity profiles which are assimilated producing initial conditions for numerical weather predictions. In addition, this analysis of the HIRS2/MSU data produces the following fields: total ozone burden of the atmosphere; sea/land surface temperature and their day-night differences, which over land can be related to soil moisture; the radiatively effective fractional cloud cover and cloud top pressure and their day-night differences; and ice and snow-cover derived from the surface emissivity at 50.3 GHz and the surface temperature. The sounding products have been used

together with a radiative transfer model, to compute outgoing longwave radiation and longwave cloud radiative forcing which show good agreement with measurements from ERB (Wu and Susskind, 1989). We have also found that the products can be used, with moderate success, to estimate precipitation. The techniques to determine total O<sub>3</sub> and estimate precipitation from the observation are not yet published and will be described briefly below.

### 5.1 Retrieved Total Ozone Burden

The ozone retrieval is performed as part of the retrieval process after the surface temperature and atmospheric temperature-humidity profile have been determined. Using these parameters and a first guess ozone profile,  $O_3^o(P)$ , which is taken from a zonally averaged climatology, the brightness temperature  $\Theta_9^o$  is computed (channel 9 is the HIRS2 9.6  $\mu\text{m}$  channel sensitive to ozone). This brightness temperature is then compared to the cloud corrected observation in channel 9,  $\hat{\Theta}_9$ , and the ozone profile is modified according to the difference between the computed and observed brightness temperatures, and the sensitivity of the brightness temperature calculation to changes in the total ozone. The retrieved ozone profile,  $O_3(p)$ , is scaled according to

$$O_3(p) = O_3^o(p) [1 + a] \quad (1)$$

where

$$a = 0.3 (\hat{\Theta}_9 - \Theta_9^o) / [\Theta_9^{(.3)} - \Theta_9^o] \quad (2)$$

and  $\Theta_9^{(.3)}$  is the brightness temperature computed when the initial ozone profile is multiplied by 1.3 everywhere. Total O<sub>3</sub> is not retrieved if either the temperature profile for that location has already been rejected or the sensitivity of the brightness temperature to changes in total O<sub>3</sub> is less than 1°C for a change of 40 Dobson units.

Total ozone is affected to first order by two quantities, the distribution of the mixing ratio of O<sub>3</sub> in the stratosphere, which is O<sub>3</sub>

HIRS/MSU RETRIEVED OZONE (DOBSON UNITS)  
DECEMBER 3, 1978

AREA MEAN = 279.87 STANDARD DEV = 49.51

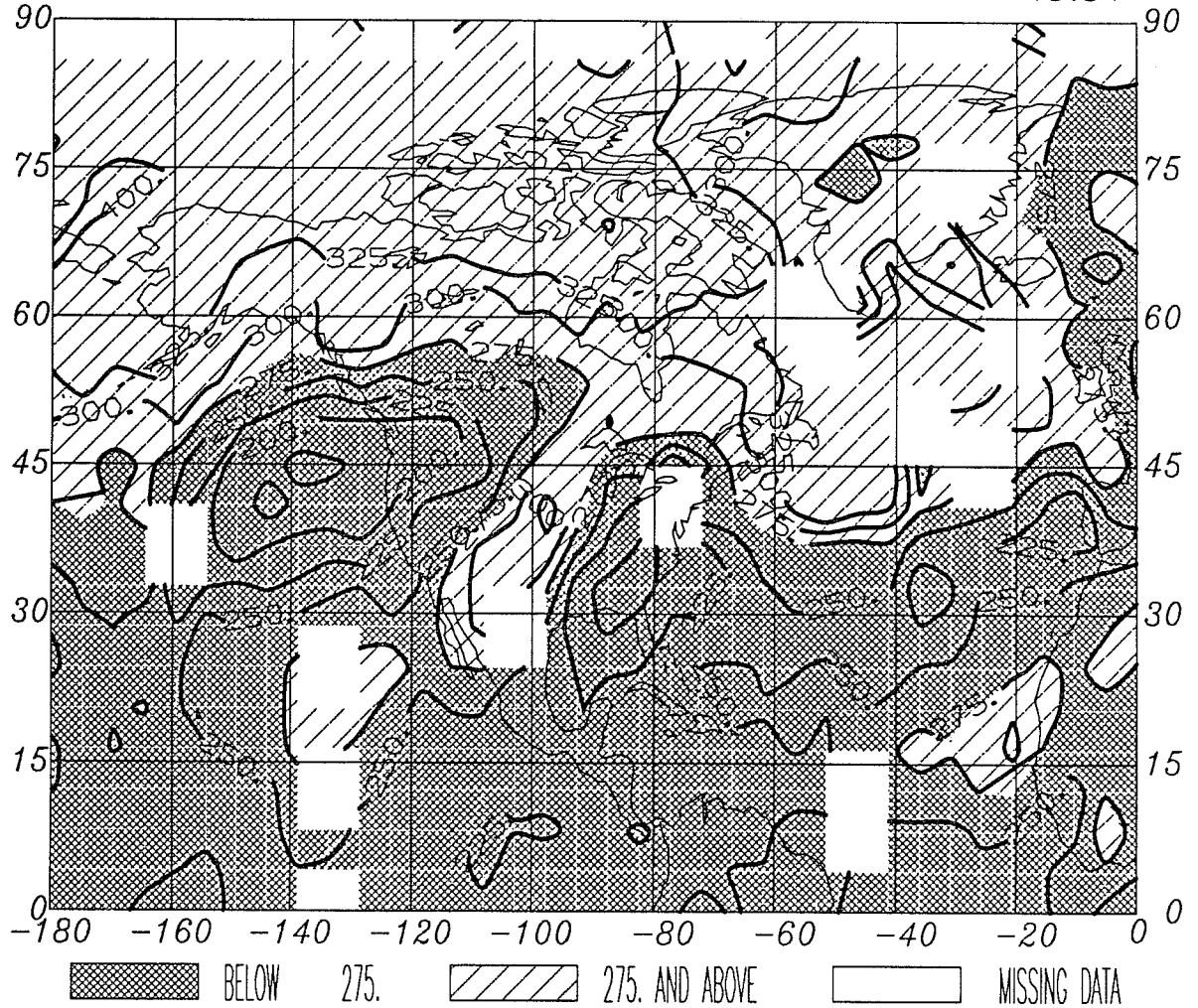


Figure 6 Total ozone (Dobson Units) retrieved for the period Dec. 3, 1978, 12Z  $\pm$ 12 hours, plotted on a 4°x5° grid.



HIRS/MSU RETRIEVED 500 - 1000 MB THICKNESS  
DECEMBER 3, 1978

AREA MEAN = 5413.43 STANDARD DEV = 270.25

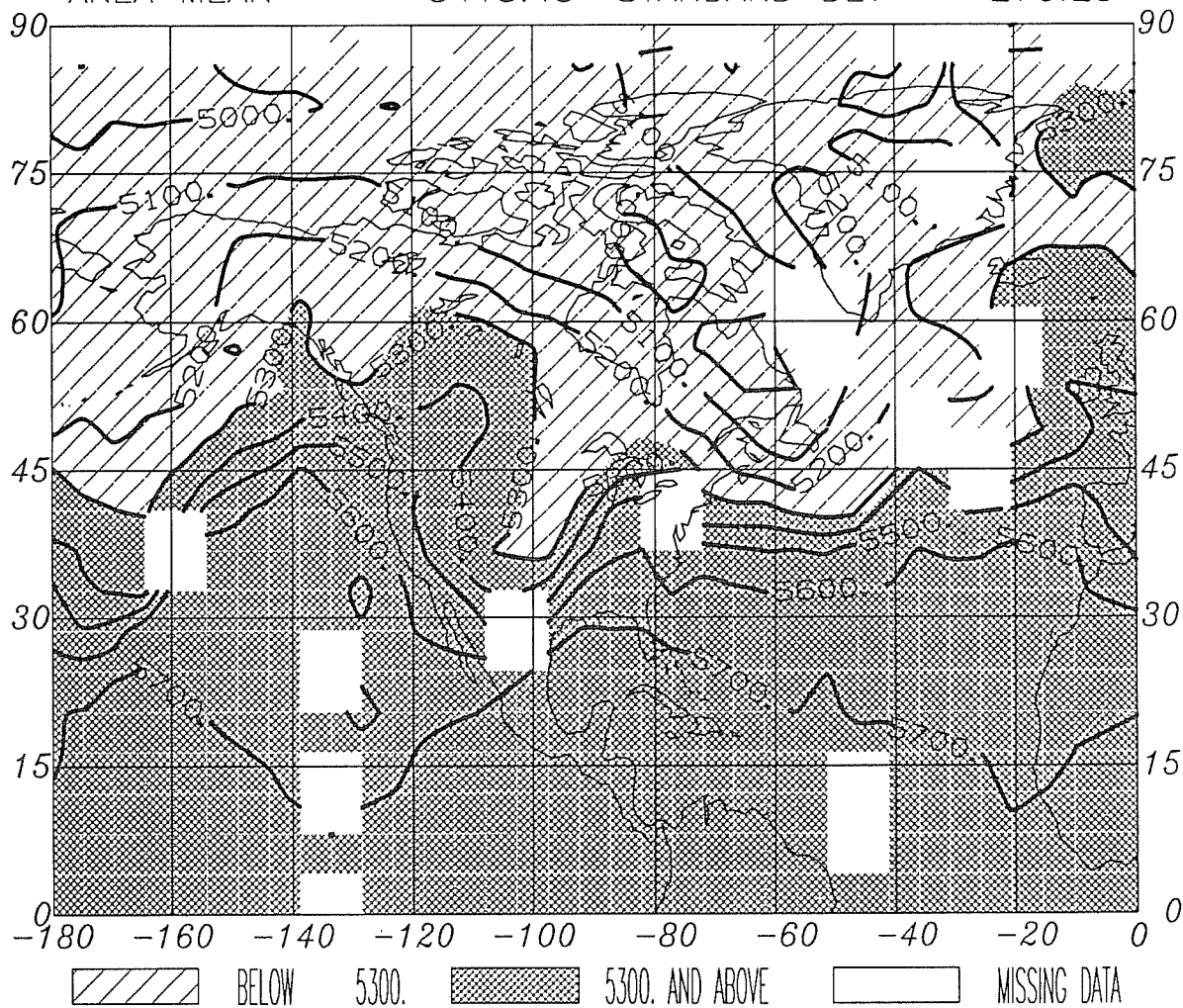


Figure 7 500 - 1000 mb thickness (meters) retrieved for the period Dec. 3, 1978 12Z ±12 hours, plotted on a 4°x5° grid.

rich, and the depth of the stratosphere, which is given by the tropopause pressure. Low values of the tropopause pressure, indicating a shallow stratosphere, correspond to low total O<sub>3</sub> values. Thus to first order, the total O<sub>3</sub> field appears to be more a measure of tropospheric circulation than of stratospheric photo-chemical processes.

## 5.2 Examples of Single Day Fields

Figure 6 shows the total ozone retrievals for December 3, 1978, 12Z  $\pm$ 12 hours, averaged on a 4 by 5 degree grid. Areas with less than 275 Dobson units of O<sub>3</sub> are shaded in the darker pattern, and areas of missing data (no retrieval performed) are left blank in the picture. It is apparent that tropical air has lower total O<sub>3</sub> than polar air. This results primarily from the reduction in the depth of the stratosphere in tropical air. More significant is the ability to identify and distinguish air mass types from the O<sub>3</sub> field. Note, for example, the sharp incursion of polar air in a northeast southwest orientation throughout the central United States, and the incursion of a tropical air mass at the northeastern edge of the scene.

Figure 7 shows the satellite retrieved 500-1000 mb thickness field for the same period. Values greater than 5300 meters are shaded. This very coherent field is the type of data which entered into the interactive assimilation, and was produced with no analysis procedure other than averaging the retrieved values in a grid box and contouring the resultant values. Comparison of Figures 6 and 7 show very good qualitative agreement, with low O<sub>3</sub> values corresponding to warmer air. The circulation appears to be depicted more clearly and sharply in the O<sub>3</sub> field than in the thickness field however. It is apparent that this could represent a powerful analysis tool if properly used.

Figure 8 shows the retrieved total precipitable water for the same period. This field is again qualitatively similar to those in Figures 6 and 7 and is especially useful for depicting the incursion of moist tropical air into the extra-tropics. We have not yet attempted to assimilate this data into the model however.

Figure 9 shows the retrieved cloudiness for the same time period. Cloud retrievals are performed under all conditions. Successful

atmospheric soundings can be performed under most cloud conditions. One can observe a correlation of some of the areas of rejected retrievals with areas of cloud fraction greater than 75% however. It should be borne in mind in examining these figures that they all represent the average of data from 2 satellite passes, 12 hours apart.

### 5.3 Global Precipitation Estimate

A new technique has been developed to estimate precipitation, on a global domain, using products determined from HIRS2/MSU sounding data. Although none of the channel radiances from these instruments are directly sensitive to precipitation, the radiances are sensitive to a number of geophysical parameters which are determined from analysis of the data. We have found that these products can be used, with moderate success, to estimate precipitation. Currently, the algorithm estimates precipitation based on the cloud top pressure, effective cloud fraction, and temperature-humidity profile, all retrieved using a 2 x 2 array of HIRS2 spots, with a nominal 60 km resolution, depending on satellite zenith angle. Of the parameters used to estimate precipitation, the cloud top pressure and cloud fraction are the most significant.

The current algorithm assumes the estimated precipitation,  $\hat{R}$ , is proportional to cloud volume, that is,

$$\hat{R} = A\alpha(Z_c - Z_B) \quad (3)$$

where  $\alpha$  is the cloud fraction,  $Z_c$  is the cloud top height,  $Z_B$  is the height of the cloud base, and  $A$  is a proportionality constant which may depend on location and time of year.  $\alpha$  and  $Z_c$  are determined directly from the soundings but  $Z_B$  is difficult to measure. If one looks at the ratio  $\bar{R}/\bar{\alpha}\bar{Z}_c$ , where  $\bar{R}$  is averaged rain gauge measurements for a location over a period of time, and  $\bar{\alpha}$  and  $\bar{Z}_c$  are the average values of the retrieved cloud fraction and cloud top height in that area and period, it is observed that this ratio tends to be smaller in cases of low relative humidity and low cloud fraction. To roughly account for this in the form of equation (3), we let  $Z_B$  increase with decreasing relative humidity  $R_H$ , and cloud fraction  $\alpha$ , and use the form

HIRS/MSU RETRIEVED CLEAR AIR PRECIPITABLE WATER  
DECEMBER 3, 1978

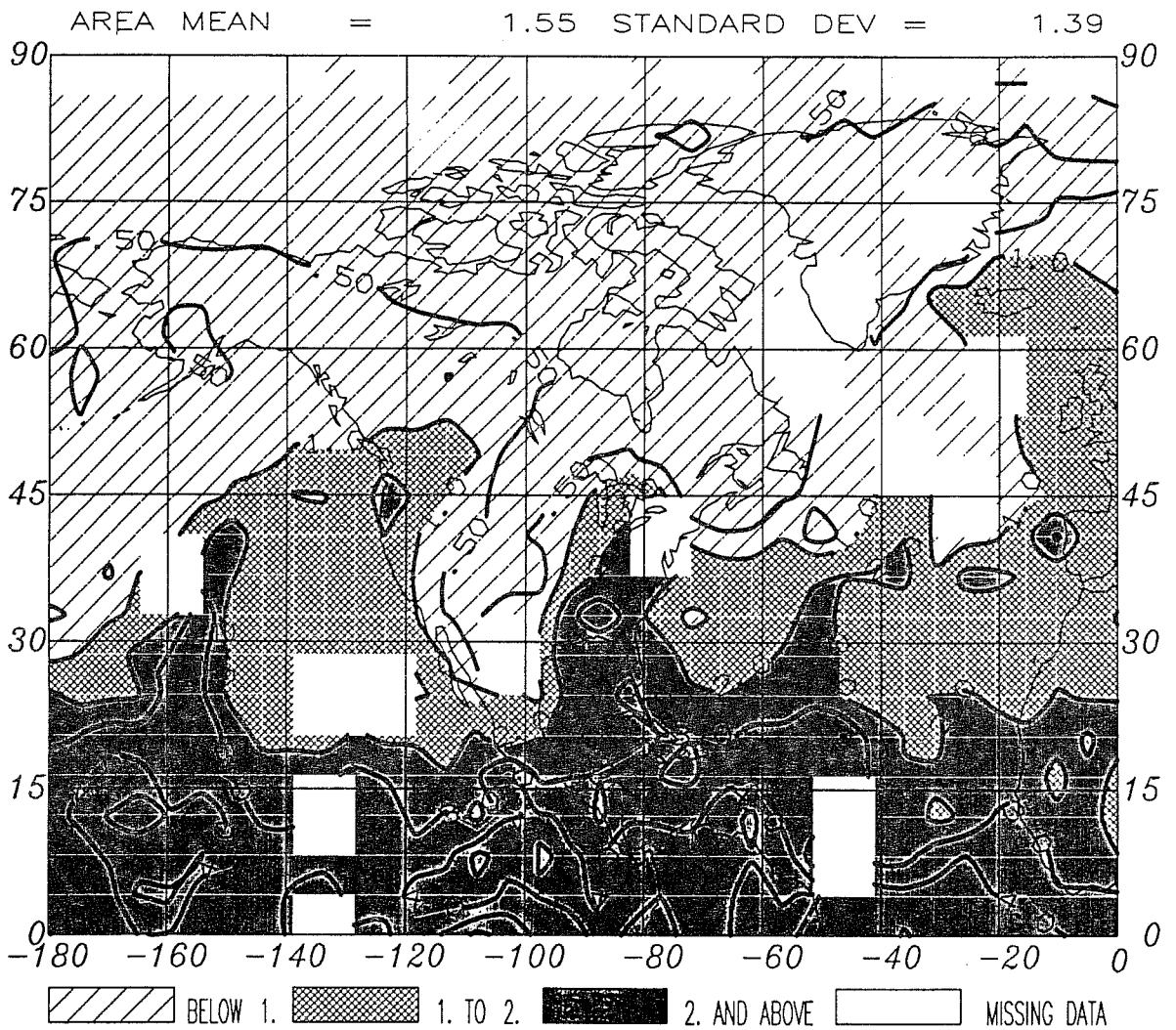


Figure 8 Clear air precipitable water (cm) retrieved for the period Dec. 3, 1978 12Z  $\pm$ 12 hours, plotted on a 4°x5° grid.

HIRS/MSU RETRIEVED EFFECTIVE CLOUD FRACTION  
DECEMBER 3, 1978

AREA MEAN = 43.16 STANDARD DEV = 23.60

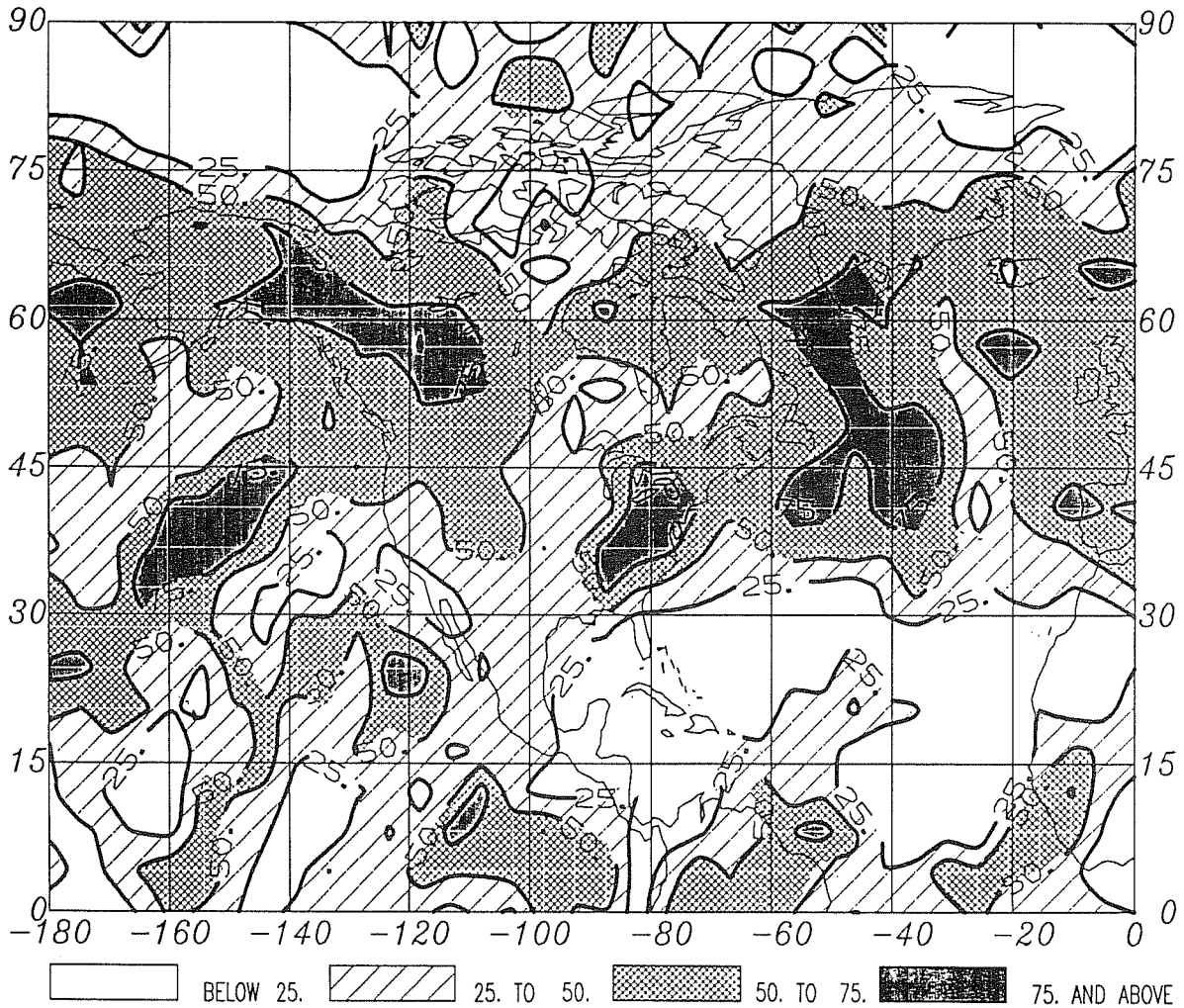


Figure 9 Effective cloud fraction (%) retrieved for the period Dec. 3, 1978 12Z ±12 hours, plotted on a 4°x5° grid.

$$\hat{R} = A_{x,y,t} \alpha [Z_c - 10(.9 - R_H) - 5(.9 - \alpha)] \quad (4)$$

where  $R_H$  is the average relative humidity between the surface and 500 mb, and  $A$  is in (mm/day)  $\text{km}^{-1}$ . Precipitation estimate is determined for all scenes, as are cloud parameters, with first guess temperature-humidity profiles being used in equation (4) if the retrievals have been rejected.  $\hat{R}$  is taken as zero if either  $\alpha$  is zero or the expression in the brackets is less than or equal to zero. This occurs a majority of the time. Using the form of equation (4), we have determined a simple form of  $A$ , which when used in equation (4), gives good agreement with 12000 values of monthly mean global rain gauge measurements throughout the FGGE year, 1979.  $A$  is different for land and ocean and has a small dependence on latitude and time of year. The correlation of estimated and measured precipitation is 0.78 for the ensemble with an RMS difference of 1.7 mm/day.

Fields in general show very good agreement with global rain gauges on 10 day, monthly, and annual time scales, and show good agreement in inter-month differences as well. While most rain gauges are over land, the precipitation estimate fields are global and show how patterns over land are connected to each other via patterns over the oceans. There is a tendency to damp variations somewhat compared to rain gauge measurements however. Research is currently underway to determine methods to distinguish large scale from convective precipitation and to model these separately.

Daily fields of precipitation estimate may also prove useful for analysis purposes. Figure 10 shows the precipitation estimate for December 3 based on 24 hours of data. Values more than 3 mm/day are indicated in the figure. There is of course some correlation of rain with cloudiness, shown in Figure 9, but most clouds are thought not to be precipitating according to the algorithm. Examination of Figure 10 reveals that the regions of more intense precipitation in mid latitudes seem realistic with respect to their intensity, spatial extent and placement. Comparison of Figure 10 with the synoptic scale flow, as indicated by either the total ozone map of Figure 6 or the analyzed 500-1000 mb thickness in Figure 7, shows the centers of intense precipitation to be correctly located along the leading edges of the

HIRS/MSU PRECIPITATION ESTIMATE (MM/DAY)

DECEMBER 3, 1978

AREA MEAN = 2.39 STANDARD DEV = 3.64

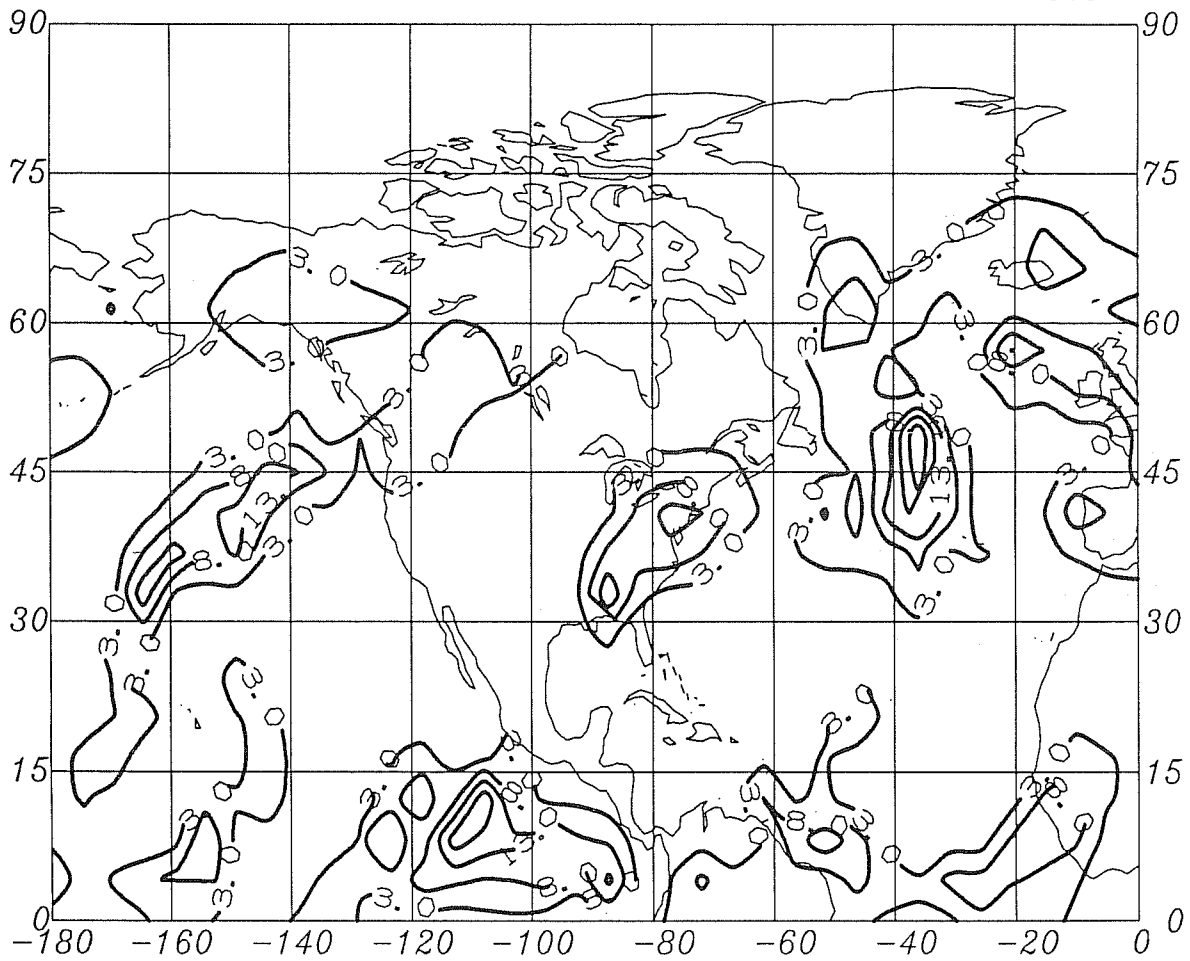


Figure 10 Precipitation estimate (mm/day) from HIRS2/MSU soundings for the period Dec. 3, 1978, 12Z  $\pm$ 12 hours, plotted on a 4 $\times$ 5 $^\circ$  grid.

cold troughs. This result is less apparent for the intense precipitation centered at 46N, 39E, because retrievals are missing in this area. The data gaps are in fact most likely the results of the precipitation itself, together with the extensive cloudiness, which caused the retrievals to be rejected. There are hints of a tropical air mass to the east of this area of precipitation in each of the O<sub>3</sub>, 500-1000 mb thickness and precipitable water fields, however.

## 6. FUTURE PLANS

The results shown in this paper are very encouraging from the point of view of improving forecast skill by utilization of satellite data. Nevertheless, all tests thus far have been made using an old analysis technique (SCM) in conjunction with a rather coarse (4° x 5°) 9 level model. We are currently implementing an improved version of the model that will be run at 2° x 2.5° spatial resolution with 15 vertical levels and improved physical parameterizations. We are also optimizing a new optimal interpolation analysis scheme for use with this model in the interactive analysis mode. It is expected that the new system will produce not only improvements in overall forecast skill, but also result in additional impact of satellite data on forecast skill, as was found when forecasts were run on the 2° x 2.5° version of the 9 level model, because a better system can take better advantage of the satellite data.

Along similar lines, we are conducting a joint test with NMC. In the first step, non-interactive retrievals will be run at GLA using the operational NMC 6-hour forecast first guess run for the period May 15-July 15, 1988. These retrievals will be sent to NMC as input data for a non-real-time forecast assimilation cycle experiment, with forecast skill being compared to that which had been obtained with the operational cycle. In addition, the possible utility of the additional satellite derived fields will be studied. If the results look encouraging, the possibility of implementing an interactive analysis cycle at NMC will be examined and pursued.

The concept of "interactive" retrievals raises a very intriguing question: Must every institution producing forecasts generate their own satellite retrievals in conjunction with their own model to obtain best results? Our suspicion is that the answer to this question is not



necessarily. The GLA retrieval system gives results which do not depend significantly on the first guess used. We feel that use of a reasonably accurate first guess from any good GCM should produce basically the same retrievals and hence contain comparable utility for assimilation purposes. To try to answer this question, we will compare the retrievals generated using the NMC forecast guess with those generated interactively using our own model for the same period. In addition, we will also assimilate the retrievals generated using the NMC guess into our own model and test the impact on forecast skill.

#### References:

- Atlas, R., M. Ghil and M. Halem, 1982: The effect of model resolution and satellite sounding data on GLAS model forecasts. Mon. Wea. Rev., 110, 662-682.
- Baker, W. E., 1983: Objective analysis and assimilation of observational data from FGGE. Mon. Wea. Rev., 111, 328-342.
- Baker, W. E., R. Atlas, M. Halem and J. Susskind, 1984: A case study of forecast sensitivity to data and data analysis techniques. Mon. Wea. Rev., 112, 1544-1561.
- Baker, W., S. C. Bloom, J. S. Woollen, M. S. Nestler, E. Brin, T. W. Schlatter and G. W. Branstator, 1987: Experiments with a three-dimensional statistical objective analysis scheme using FGGE data. Mon. Wea. Rev., 115, 273-296.
- Charney, J., M. Halem, and R. Jastrow, 1969: Use of incomplete historical data to infer the present state of the atmosphere. J. Atmos. Sci., 26, 1160-1163.
- Ghil, M., M. Halem, R. Atlas, 1979: Time-continuous assimilation of remote-sounding data and its effect on weather forecasting. Mon. Wea. Rev., 107, 140-171.
- Kalnay, E., R. Atlas, W. Baker and J. Susskind, 1985: GLAS experiments on the impact of FGGE satellite data on numerical weather prediction. International FGGE Workshop, National Academy of

Sciences, T. O'Neil (editor), Woods Hole, MA, July 2-20, 1984, 121-145.

Kalnay, E., R. Balgovind, W. Chao, D. Edlmann, J. Pfaendtner, L. Takacs and K. Takano, 1983: Documentation of the GLAS Fourth Order GCM. NASA Tech. Memo., 86064.

Reuter, D., J. Susskind and A. Pursch 1988: First guess dependence of a physically based set of temperature humidity retrievals from HIRS2/MSU data. J. Atmos. Ocean. Tech., 5, 70-83.

Susskind, J., J. Rosenfield, and D. Reuter, 1983: An accurate radiative transfer model for use in the direct physical inversion of HIRS2 and MSU temperature sounding data. J. Geophys. Res., 88, 8550-8568.

Susskind, J., J. Rosenfield, D. Reuter, and M. T. Chahine, 1984: Remote sensing of weather and climate parameters from HIRS2/MSU on TIROS-N. J. Geophys. Res., 89D, 4677-4697.

Susskind, J. and D. Reuter, 1985: Retrieval of Sea-Surface temperatures from HIRS2/MSU. J. Geophys. Res., 90C, 11602-11608.

Susskind, J., D. Reuter and M. T. Chahine, 1987a: Cloud fields retrieved from HIRS2/MSU data. J. Geophys. Res., 92D, 4035-4050.

Susskind, J., D. Reuter, W. Baker, J. Pfaendtner, and T. O. Aro, 1987b: The GLA interactive forecast-retrieval-analysis cycle for the FGGE year. FGGE Hydrological Cycle Workshop, National Academy of Sciences, F. White editor, Arlie, VA, April 27-30, 1987, 98-112.

Wu, M-L. C. and J. Susskind, 1989: Outgoing longwave radiation computed from HIRS2/MSU soundings. Submitted to J. Geophys. Res.